

# Pulse RF Operation of MEMS Capacitive Switches

Cristiano Palego<sup>#1</sup>, Jie Deng<sup>#1</sup>, Subrata Halder<sup>#1</sup>, Zhen Peng<sup>#1</sup>, James C. M. Hwang<sup>#1</sup>, David I. Forehand<sup>\*2</sup> and Charles L. Goldsmith<sup>\*2</sup>

<sup>#</sup>ECE, Lehigh University, 5 East Packer Ave, Bethlehem PA, 18015, USA

<sup>1</sup>crp207@lehigh.edu

<sup>\*</sup> MEMtronics Corp., Plano, TX 75075, USA

**Abstract** — Shifts in the pull-in voltage of electrostatically actuated MEMS capacitive switches were characterized under pulse RF excitation, which allowed the electrical and thermal effects of the RF excitation to be separated. The resulted multi-physics model accurately predicted the pull-in voltage shift under different pulse powers and duty cycles. By comparing the power capacity of switches made of aluminum or molybdenum, a new figure of merit is proposed for selecting the optimum material for the fabrication of high-power MEMS capacitive switches.

**Index Terms** — microelectromechanical devices, microwave devices, microwave switches, pulse measurement.

## I. INTRODUCTION

For phased-array radar and communications systems, RF MEMS capacitive switches are attractive mainly due to their low power consumption and high linearity [1]. However, as the RF excitation approaches the power handling capacity (typically on the order of watt) of the switches, they can nonetheless become nonlinear owing to the coupled electrical (self biasing) and thermal (self heating) effects. Using pulse RF excitation, this paper attempts to separate the electrical and thermal effects, with the aim of accurately modeling the nonlinearity and capacity of the switches under different operating conditions.

While self biasing is determined by the instantaneous pulse power only, different duty cycles would result in different amounts of temperature rise. Therefore, by measuring the reduction of the pull-in voltage of the switches under different pulse powers and duty cycles, the electrical and thermal effects can be separately extracted. This is critical because the RF current distribution hence the temperature profile is highly localized and cannot be simulated by simply raising the ambient temperature. Although the present theoretical analysis is simplified by assuming uniform heating, the present experimental technique can be used to validate finite-element analysis of coupled electrical and thermal effects in the future.

## II. EXPERIMENTAL

The pulse RF excitation has a pulse repetition frequency of 2.78 kHz and a capacity up to 2 W at 15 GHz. The duty cycle is varied from 100% down to 10% before ringing affects measurement accuracy. The switch output power is measured by using a spectrum analyzer then corrected for cabling loss.

A pulse generator is used to ensure both the RF excitation and the bias voltages are applied only during the pulse. Meanwhile, the bias voltage is stepped up by 0.25 V every 20 s until the spectrum analyzer senses an abrupt drop in the output power. The bias voltage at this point is deemed the pull-in voltage  $V_p$  of the switch.

Details of the switches under test have been published elsewhere [2]. Briefly, the switches are actuated

TABLE I  
PROPERTIES OF SWITCHES UNDER TEST

Symbol	Description	Al	Mo#1	Mo#2
$V_p$ (V)	pull-in voltage	30	23	28
$\rho$ ( $\mu\Omega\text{-cm}$ )	resistivity	2.7	5.0	
$k$ (W/cm/ $^{\circ}\text{C}$ )	thermal conductivity	2.4	1.4	
$\alpha$ (ppm/ $^{\circ}\text{C}$ )	thermal expansion coefficient	23	4.8	
$E$ (GPa)	Young's modulus	70	330	
$\gamma$	geometric factor	1.3		
$\nu$	Poisson's ratio	0.35	0.31	
$\sigma$ (MPa)	residual stress	150	84	120
$\tau_{HEAT}$ ( $\mu\text{s}$ )	heating time constant	210	150	140
$\tau_{COOL}$ ( $\mu\text{s}$ )	cooling time constant	260	180	170

electrostatically. Each switch resembles a section of 50  $\Omega$  coplanar transmission line that is fabricated on a Pyrex 7740 glass substrate with a thermal expansion coefficient  $\alpha = 3.25$  ppm/ $^{\circ}\text{C}$ . The center conductor of the transmission line forms the stationary electrode of the switch, which is overcoated with  $\text{SiO}_2$ . A bowtie-shaped membrane is suspended over the stationary electrode but fixed at both ends to the ground planes of the transmission line. The membrane has a length  $L = 320$   $\mu\text{m}$ , width  $W \approx 100$   $\mu\text{m}$ , and thickness  $t = 0.28$   $\mu\text{m}$ .

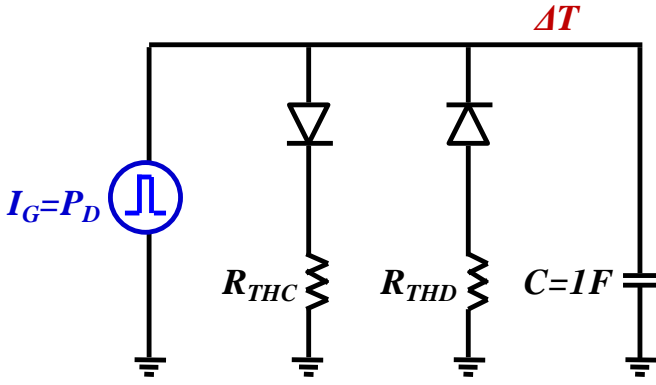


Fig. 1. Thermal equivalent circuit for calculating the temperature rise under pulse RF power.

Normally, the membrane and the stationary electrode have a coupling capacitance  $C_{OFF} = 0.1$  pF across an air gap  $g = 2.5$   $\mu\text{m}$ , which causes little impediment to the transmission of the RF signal. When the bias voltage exceeds  $V_p$ , the membrane is pulled in to contact the stationary electrode thereby increasing the coupling capacitance to  $C_{ON} = 1$  pF and shunting most of the RF excitation to ground. The switching time usually take several microseconds.

As listed in Table I, the membrane is made of either aluminum or molybdenum. The aluminum switch is packaged using a microencapsulation technique [3]; the molybdenum switches are unpackage. Although all switches have the same geometry, they have different pull-in voltages primarily due to the difference in residual stress. These switches have state-of-the-art performance and reliability, with their lifetimes limited mainly by dielectric charging [4]. Therefore, care was taken to minimize the contact time during measurements. Usually,  $V_p$  after measurements is within  $\pm 0.1$  V of the pristine value.

## II. THEORETICAL ANALYSIS

Following [5], the coupled electrical and thermal effects of RF excitation on switch operation can be analyzed. The RF voltage is rectified by the square-law dependence of the electrostatic force between the membrane and the stationary electrode and can be converted to an equivalent dc bias, which reduces the applied bias required to pull in the membrane. In addition, the RF current leaks through  $C_{OFF}$  to the membrane and causes self heating and temperature rise, which alters its material and mechanical properties such as residual stress. Both self biasing and self heating depend linearly on the RF power and their combined effect on the switch pull-in voltage is derived by the analysis below. With sufficient RF power, the coupled electrical and thermal effects can pull in the membrane without any applied bias. However, the switch may behave nonlinearly at an RF power much lower than that required for self actuation.

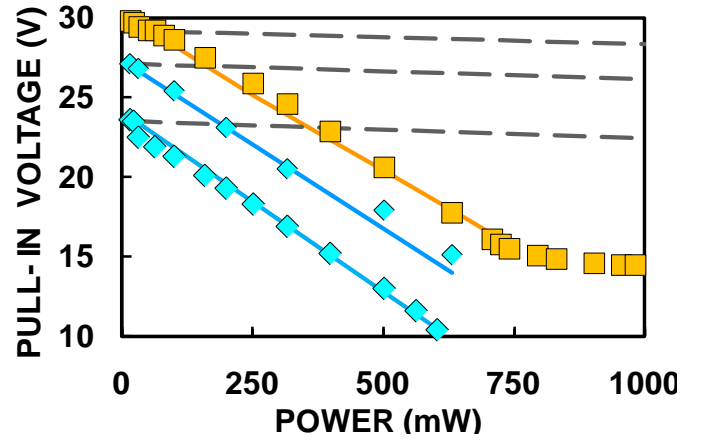


Fig. 2. Measured (symbol) vs. modeled (solid curve) pull-in voltage as a function of CW RF power for an aluminum switch ( $\square$ ) and two molybdenum switches ( $\diamond$ ), which shows how isothermal self biasing (dashed curve) is exacerbated by self heating. Although the switches have different small-signal pull-in voltages due to different residual stresses, their large-signal pull-in voltages have comparable power dependence due to comparable self heating.

As a start, the reflection by the small  $C_{OFF}$  can be neglected and the equivalent DC voltage across the switch for an RF power  $P$  is

$$V_{DC-EQ} = \sqrt{PZ_0} \quad (1)$$

where  $Z_0 = 50 \Omega$ . On the other hand, the leakage through  $C_{OFF}$  is not negligible and the power dissipated in the membrane is

$$P_D = PZ_0(\omega C_{OFF})^2 \rho L/Wt \quad (2)$$

where  $\omega$  is the angular frequency and  $\rho$  is the resistivity of the membrane. Assuming uniform current/temperature distribution and heat loss through conduction only, the temperature rise due to CW RF power is

$$\Delta T = P_D L/kWt \quad (3)$$

where  $k$  is the thermal conductivity of the membrane. Further, assuming the dominant thermal effect is on the residual stress  $\sigma$ ,

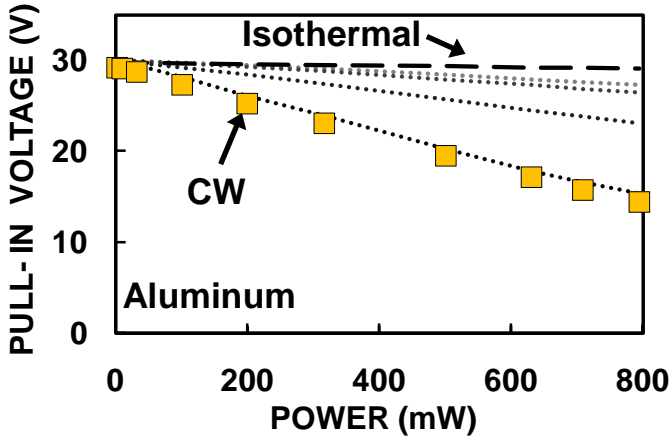
$$\Delta \sigma = \Delta \alpha E \Delta T \quad (4)$$

where  $\Delta \alpha$  is the difference in expansion coefficients between the membrane and the substrate, while  $E$  is the Young's modulus of the membrane. The pull-in voltage, taking into account the self heating and self biasing effects is

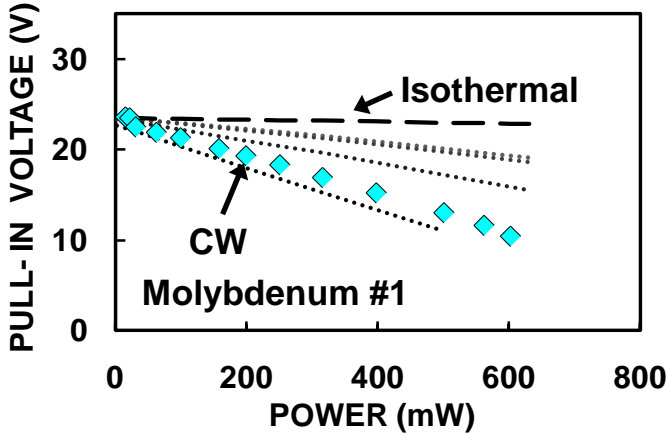
$$V_p = \sqrt{64\gamma(1-\nu)t g^3 (\sigma - \Delta \sigma) / 27 L^2 \epsilon_0 - PZ_0} \quad (5)$$

where  $\gamma \approx 1$  is a geometric factor,  $\nu$  is the Poisson's ratio, and  $\epsilon_0$  is the vacuum permittivity.

The temperature rise under pulse RF excitation cannot be easily derived. Instead, a thermal equivalent circuit similar to that of [6] is used to fit the experimental data. As shown in Fig. 1, two R-C subcircuits simulate heating and cooling, respectively, during each duty cycle. The capacitances are set to unity so that the resistances correspond directly to thermal



(a)



(b)

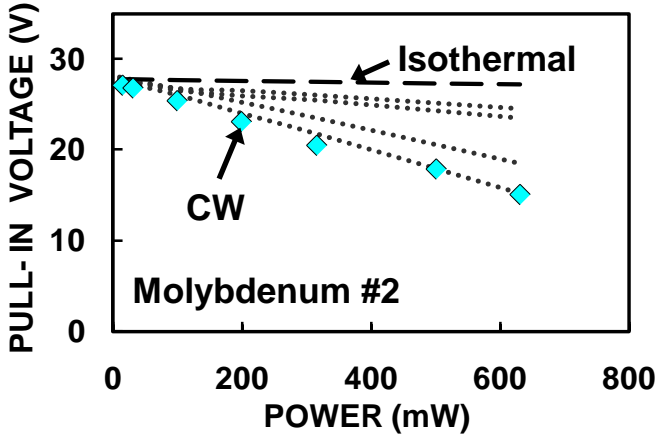


Fig. 3. Measured (dotted) pull-in voltages as functions of pulse RF power with the duty factors of 10%, 20%, 40% and 75% top down. Measured CW case (solid) and calculated isothermal case (dashed) are also included.

time constants:  $R_{THC} = \tau_{HEAT}$  and  $R_{THD} = \tau_{COOL}$ . Diodes are used in each subcircuit to direct charge (heat) flow. The capacitor is charged through  $R_{THC}$  when the RF power is pulsed on and discharged through  $R_{THD}$  when the RF power is off. The resulting voltage across the  $R$ - $C$  subcircuits represents  $\Delta T$ .

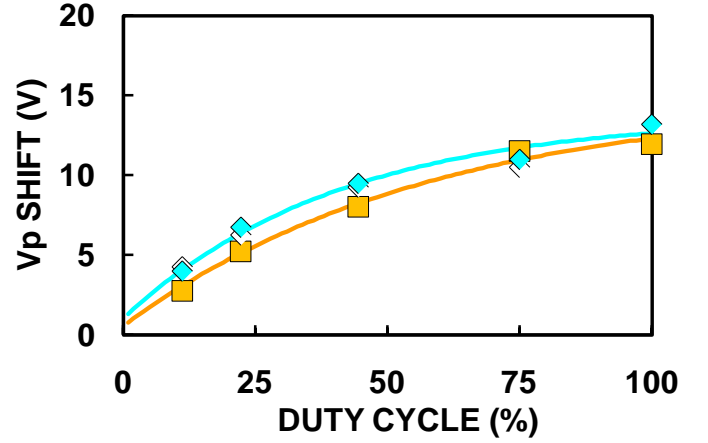


Fig. 4. Measured (symbols) vs. modeled (curve) duty-cycle dependence of pull-in voltage shift for the aluminum (□) and molybdenum (♦) switches under a pulse RF power of 630 mW.

### III. RESULTS AND DISCUSSION

The superposition of electrical and thermal effect is illustrated in Fig. 2 for the pull-in voltage of the aluminum switch measured under different CW RF powers. It can be seen that although the two terms of (5) both depend on the square root of the RF power, the combined behavior is essentially linear up to 700 mW. Beyond 700 mW, the on and off powers of the switch output are so close to each other that the pull-in voltage cannot be reliably measured. The linear power dependence covers the range before the pull-in voltage is halved. This range is then used to test all switches under pulse RF excitation.

Fig. 3 shows the measured pull-in voltage as a function of pulse RF power with duty cycle as a parameter. Similar to the CW case of Fig. 2, the pull-in voltage appears to decrease linearly with power, but the slope is increasingly steeper with increasing duty cycle. For comparison, Fig. 2 includes the CW case as well as the isothermal case when  $V_p$  is reduced only by  $V_{DC-EQ}$  ( $\Delta\sigma = 0$ ). It can be seen that with increasing duty cycle, the pulse case approaches the CW case. However, with decreasing duty cycle, the pulse case converges at a value somewhat lower than the isothermal case. Currently, it is not clear why this discrepancy exists.

Using a combination of ideal material properties and experimentally fitted thermal properties as discussed in Sec. II, Fig. 4 shows that the pull-in voltage shift under a pulse RF power of 630 mW can be well fitted for both the aluminum and molybdenum switches. Comparable agreement is also achieved at other pulse RF powers. The extracted thermal time constants as listed in Table I are in general agreement with that estimated in [5]. These thermal time constants will be further validated at different pulse repetition frequencies and duty cycles.

#### IV. CONCLUSION

Although the aluminum and molybdenum switches have different material properties and initial  $V_p$  values, their pull-in voltages exhibit similar power dependence as shown in both Fig. 3 and Fig. 4. This implies that they have comparable power capacity. The molybdenum switches have been shown [2] to be more robust against ambient temperature change, which was attributed to the lower  $\Delta\alpha E$  product of molybdenum than that of aluminum. However, as discussed in Sec. II, power capacity is limited by the coupled electrical and thermal effects and the product of  $\rho\Delta\alpha E/k$  maybe a better figure of merit for high power material. In this case, the higher electrical and thermal resistances of molybdenum can more than compensate for its lower  $\Delta\alpha E$ . Notice that the present analysis is based on many simplifying assumptions and Table I includes only ideal bulk values. Therefore, whether aluminum or molybdenum ultimately gives higher power capacity can only be determined through more detailed theoretical analysis and experimental characterization.

#### ACKNOWLEDGEMENT

This work is supported in part by the US Defense Advanced Research Projects Agency under the Harsh

Environment, Robust Micromechanical Technology (HERMIT) Program (Contract No. F33615-03-C-7003).

#### REFERENCES

- [1] L. Dussopt, and G. M. Rebeiz, "Intermodulation distortion and power handling in RF MEMS switches, varactors, and tunable filters," *IEEE Trans. Microwave Theory Techniques*, vol. 51, pp. 1247-1256, Apr. 2003.
- [2] C. L. Goldsmith, D. I. Forehand, D. Scarbrough, I. Johnston, S. Sampath, A. Datta, Z. Peng, C. Palego, and J. C. M. Hwang, "Performance of molybdenum as a mechanical membrane for RF MEMS switches," *IEEE MTT-S Int. Microwave Symp. Dig.*, June 2009.
- [3] D. I. Forehand, and C. L. Goldsmith, "Wafer level micro-encapsulation," *Proc. Government Microcircuit Applications Critical Technology Conf.*, pp. 320-323, Apr. 2005.
- [4] C. L. Goldsmith, D. I. Forehand, Z. Peng, J. C. M. Hwang, and J. L. Ebel, "High-cycle life testing of RF MEMS switches," *IEEE MTT-S Int. Microwave Symp. Dig.*, pp. 1805-1808, June 2007.
- [5] J. R. Reid, L. A. Starman, and R. T. Webster, "RF actuation of capacitive MEMS switches," *IEEE MTT-S Int. Microwave Symp. Dig.*, pp. 1919-1922, June 2003.
- [6] X. Yuan, Z. Peng, J. C. M. Hwang, D. I. Forehand, and C. L. Goldsmith, "A transient SPICE model for dielectric charging effects in RF MEMS capacitive switches," *IEEE Trans. Electron Devices*, vol. 53, pp. 2640-2648, Oct. 2006.